IEEE Access
Multidisciplinary | Rapid Review | Open Access Journal

Received 21 June 2023, accepted 13 July 2023, date of publication 1 August 2023, date of current version 9 August 2023.

Digital Object Identifier 10.1109/ACCESS.2023.3300868

RESEARCH ARTICLE

Prediction Model for the Stored-Grain Situation Risk Point Based on Broad Learning Network

LIAN FEIYU, QIN YAO, AND FU MAIXIA
Key Laboratory of Grain Information Processing and Control, Ministry of Education, Henan University of Technology, Zhengzhou 450001, China
College of Information Science and Engineering, Henan University of Technology, Zhengzhou 450001, China

Corresponding author: Fu Maixia (fumaixia@126.com)

This work was supported in part by the Open Fund of the Key Laboratory of Grain Information Processing and Control under Grant KFJJ-2021-103, in part by the Key Scientific Research Project Program of Universities of Henan Province under Grant 22A510014, and in part by the Henan Province Colleges and Universities Young Backbone Teacher Funding Program under Grant 2020GGJS084.

ABSTRACT An accurate prediction for the stored-grain situation is a necessary means to ensure grain security. It is difficult for traditional machine learning methods to process large-scale stored-grain monitoring data, while deep learning methods have the problems of difficult model training and high resource consumption. To solve these problems, a risk prediction model for stored-grain situations was proposed based on a broad learning network. First, the concept of stored-grain risks was proposed and defined in three categories: low, medium, and high. Then, based on the existing broad learning network, two improved broad learning algorithms were proposed: an enhanced node incremental algorithm and an input data incremental algorithm. Based on the multi-modal features of stored-grain situation data, canonical correlation analysis is introduced to the feature extraction and fusion methods. Finally, an accurate prediction model of stored-grain risk based on improved broad learning and correlation analysis is constructed. The experimental results show that, compared to the traditional broad learning model, the two improved broad learning models improve the accuracy of stored-grain risk prediction by more than 2.3%. Meanwhile, compared with the existing deep learning models, the improved broad learning model reduces training time by more than 20 times without reducing the prediction accuracy and has better robustness. In short, the incremental learning training method can make the prediction accuracy of the broad learning model close to or reach the level of the deep learning model with the increase of training data, which proved that the proposed methods may be an effective alternative to deep learning models.

INDEX TERMS Stored-grain risk point, broad learning network, multi-modal data, incremental learning, canonical correlation analysis.

I. INTRODUCTION

Grain reserves are an important measure to guarantee food security in a country. To ensure the safety of grain storage, it is also necessary to predict the changing trend of the grain storage situation in time, in addition to real-time monitoring of the state of grain storage. However, relevant studies have shown that the prediction of the stored-grain situation is a very complex problem [1] and is also a key scientific and technological problem that needs to be solved urgently in the field of grain storage. To facilitate this research, we put forward the concepts of ''dangerous grain situation'' and ''stored-grain situation risk point,'' and researched the ''stored-grain situation risk point prediction model.'' This model predicts a time point at which the stored grain will be in a dangerous state (refers to mildew or deterioration of quality). The prediction accuracy of the stored-grain situation risk points is related to many factors, such as grain variety, granary type, local storage conditions, meteorological conditions, geographical location, grain temperature, and humidity, initial moisture content of the grain, impurity content of the grain, gas composition in the warehouse, and types and the initial state of biological harmful factors. Because of the complex interactions among various factors,

The associate editor coordinating the review of this manuscript and approving it for publication was Varuna De Silva.

it is very difficult to predict the risk point of a stored-grain situation.

Prediction methods based on traditional machine learning include linear regression (LR), nonlinear regression, Markov method, support vector regression (SVR) [2], random forest [3], ARIMA [4], grey prediction models [5], and BPNN [6]. These methods are widely used in various fields. However, data on stored-grain situations are very complex, including static, dynamic, one-dimensional, two-dimensional, and three-dimensional data. The amount of data is large and the attributes and characteristics of the data are diverse. It is difficult for prediction models based on traditional machine learning methods to effectively process a large amount of stored-grain situation data from multiple sources. As a result, this type of forecasting model can only use partial data to make one-sided predictions of the stored-grain situation, which is poor in meeting the actual needs of ''grain situation risk-point prediction. At present, deep learning algorithms have been greatly developed and widely used, and their outstanding advantage is that they can independently learn the deep features in samples and can greatly improve the model prediction performance. Thus, it is a good choice for constructing a prediction model for the risk point of the stored-grain situation. [7], [8]

When faced with big data, deep learning models need to learn a large number of weight parameters, and because of the greater number of intermediate layers in deep learning networks, the application of the BP algorithm in the training of deep neural networks is not only very time-consuming but also easily encounters the problem of gradient disappearance or gradient explosion. Stored-grain situation data are big data, and these data not only possess high dimension and large scale but also possess dynamic growth trends, which undoubtedly bring great difficulties to the training of stored-grain situation risk-point prediction models using deep learning. Therefore, it is necessary to propose a new neural network model that is simple and easy to train and can adapt to modeling and training using large-scale dynamic stored-grain situation data to ensure model accuracy.

The introduction of broad learning [9], [10], [11] makes it theoretically possible to generate such neural network models. Neural networks that adopt a broad learning mode are called broad-learning networks (BLN). Based on the original shallow neural network, it expands the network along the width direction and the hidden layer into a cascade structure composed of feature nodes and enhanced nodes. Ridge regression of the pseudo inverse is designed to find the desired connection weights, which is significantly faster than the solving speed of the gradient descent method. Simultaneously, the broad learning network can also adopt the incremental learning method to be updated quickly [12]. Owing to the advantages of a broad learning network, it has received significant attention since it was proposed and has been successfully applied in image classification [13], [14], pattern recognition [15], fault detection [16], disease diagnosis [17], and other fields.

In this study, a new stored-grain situation risk prediction model is proposed based on the basic theory of broad learning. The main contributions of the study are as follows:

(1) A simple broad learning neural network structure is proposed, and a training method based on incremental learning is introduced, which greatly reduces the complexity of the model and training time.

(2) Through experiments, it is proved that the prediction accuracy of the model can approach or even reach the prediction level of the deep learning model through incremental learning, and it can accurately predict the changes in storage grain conditions within a month. Our research shows that in some prediction fields, such as the one studied in this paper, our proposed model can be an effective alternative to the deep learning model.

II. RELATED WORKS

At present, the risk warning to stored grain is mainly realized by establishing a mathematical model. The main models include the empirical model, mass-heat transfer model, and machine learning model [18]. Due to the implementation of the grain reserve system in China, there are more and higher levels of research in this field.

The empirical models include the power function model, exponential function model, and sine function-based model. The model based on the sine function is summarized according to the grain situation data of large granaries in China, as shown below.

$$T = b + A \sin\left(x \cdot \frac{2\pi}{365} - \omega\right),$$

where b is the average temperature of the granary, A is the magnitude of the temperature change, ω is the initial phase, and x is the number of days.

During grain storage, complex ecosystems are established within the granary, with internal heat, mass, and momentum transfers. Based on this, the material transfer model, momentum transfer model, and heat transfer model are established, namely the so-called ''three-transfer'' model. Based on the three-transfer model, Quemada et al. [19] studied the influence of airflow on heat and water in the process of grain storage by analyzing the flow pattern, isotherm, and water distribution changes. REN et al. [20] established a three-dimensional numerical model of temperature change by applying the porous medium model and the solar radiation model and studied the relationship between grain pile temperature and wall temperature, grain pile height, and the distance between grain pile and wall. Yin et al. [21] built a coupled mathematical model of the temperature field, humidity field, and micro airflow field of wheat pile based on the multi-field coupling theory to simulate and predict the process of grain pile temperature change. Liu et al. [22] revealed the spatio-temporal coupling relationship between the temperature field, humidity field, and grain mold by simulating the phenomenon of mildew heating caused by a high local moisture content of corn pile.

With the rapid development of artificial intelligence, it is more accurate to use machine learning algorithms for analysis and modeling. Duan et al. [8] used temperature sensors to measure and collect grain temperature data for 423 days from a real-world granary and collect the corresponding meteorological data from China Meteorological Data Network. This paper proposes to leverage meteorological data to predict the average temperature of the grain pile with machine learning algorithms: a support vector regression (SVR) approach and an adaptive boosting (AdaBoost) approach. Li et al. [23] proposed the Holt-Winters model that is applied to the analysis and prediction of the temperature time series of the grain warehouse. The model's value is adjusted by improving the membership function and considering the influence of nearest neighbor and global data. This model is proven to perform better than the ARIMA model. Wang et al. [24] proposed the HCM model based on Fourier analysis. The model realizes the prediction of grain temperature by atmospheric temperature. Its root mean square error (RMSE) is between 1.6 and 2.3°C, which can meet the basic application requirements.

In recent years, deep learning has been gradually applied in the prediction of stored grain conditions. Wu et al. [25] aimed at temperature changes caused by heat accumulation inside grain piles, designed and trained a bidirectional LSTM neural network using the existing temperature data to accurately predict the temperature at a certain time. The experimental results show that the bi-directional LSTM neural network has a better temperature change trend than the LSTM neural network, RNN neural network, bi-directional RNN neural network, GRU neural network, and bidirectional GRU neural network has the better predictive ability. Duan et al. [26] proposed a coding-decoding model with an attention mechanism to accurately predict grain temperature. Feng et al. [27] established a grain pile temperature prediction model based on the LSTM network by converting historical grain situation data into a sparse matrix and using the Adam optimization algorithm for parameter optimization. The model can predict the temperature of the grain pile for the next 15 days.

In the risk prediction of stored-grain situations, most of the existing prediction models aim at a single-grain situation parameter, among which the most important grain situation prediction parameter is temperature. However, the prediction of temperature can only reflect the risk of the grain situation to a certain extent, and cannot reflect the risk state of the grain situation accurately. In addition, the stored-grain situation risk prediction model based on deep learning still has some problems, such as a complex model and long training time.

In this paper, a new neural network structure is proposed to overcome the shortcomings of deep learning model in the prediction of grain storage risk. The neural network follows the shallow structure of the traditional neural network, extends the input layer and the hidden layer to the breadth direction, and introduces the incremental learning mode. The new neural network can not only guarantee the same prediction accuracy as deep learning, but also greatly reduce the complexity and training difficulty, and improve the robustness. In some application areas where sample data is insufficient, it can effectively replace deep learning models.

III. BROAD LEARNING NETWORK

A. BASIC NETWORK STRUCTURE

A broad learning network (BLN) is generated based on RVFLNN (Random Vector Function Chain Neural network (RVFLNN) [28]. The network structure is shown in Fig. 1. The BLN network structure still follows the traditional shallow neural network with a three-layer structure, and the difference between them is that the BLN expands its hidden layer in the width direction; that is, the hidden layer consists of multiple groups of feature nodes and enhancement nodes. The input data X of the BLN is not directly connected with the feature node but is used as the value of the feature node after some mapping.

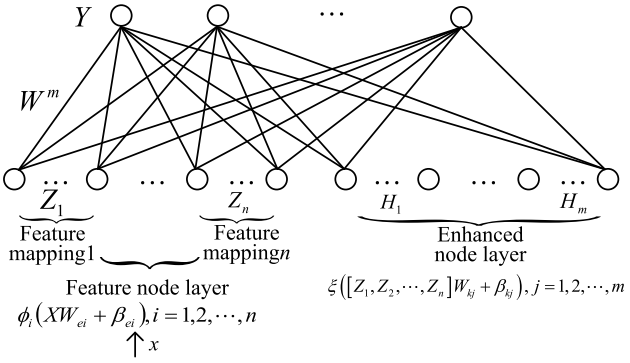

FIGURE 1. The basic structure of broad learning network.

B. INPUT LAYER

In the BLN input layer, the number of neurons is equal to the number of attributes of the input data. Assuming that the input data have M attributes, the i*th* input data can be represented as a vector $x_i = (x_{i1}, x_{i2}, \ldots, x_{iM}) \in R^M$. Assuming that there are N such input data, N M-dimensional input vectors can be represented by a matrix $X = (x_1, x_2, \ldots, x_i, \ldots, x_N)^T \in R^{N\times M}$. After batch processing of input data X, the BLN sends them to the feature nodes for transformation. Because the attributes of the input data are of different types, the raw input data are generally normalized for convenience.

C. HIDDEN LAYER

1) FEATURE NODE

According to the basic structure of the BLN shown in Fig. 1, the hidden layer comprises a feature node layer and an enhancement node layer. Assuming that the feature node layer of BLN is composed of n groups of nodes $Z_1, Z_2, \ldots, Z_n$, and the node of group Z_i is composed of q neurons, the input data X are expressed as follows after the feature mapping Z_i.

$$Z_i = \varphi_i(XW_{ei} + \beta_{ei}),\ i = 1, 2, \ldots, n. \tag{1}$$

φ_i in Eq. (1) is the activation function, and the common sigmoid and ReLU functions can be used. The activation functions for each mapping group may differ. $W_{ei} \in R^{M\times q}$ is a weight matrix of the network, and the initial value may be randomly generated. $\beta_{ei} \in R^{N\times q}$ is a bias matrix and the initial value is random. These two matrices are fine-tuned by the sparse auto-encoder to extract sparser features from the input data.

2) ENHANCEMENT NODE

The enhancement node layer of the BLN is denoted by $H_1, H_2, \ldots, H_m$. Assuming that the *jth* enhanced node H_j contains r neurons, the matrix Z^n from the feature node layer can be transformed after the enhancement node layer as follows:

$$H_j = \xi_j(Z^n W_{hj} + \beta_{hj}),\ j = 1, 2, \ldots, m. \tag{2}$$

In Eq. (2), ξ_j is the activation function, and functions such as the sigmoid function and ReLU can be used. $W_{hj} \in R^{nq\times r}$ is the weight matrix, $\beta_{hj} \in R^{N\times r}$ is the bias matrix, and their initial values are set to random values.

D. OUTPUT LAYER

The output layer of the BLN handles both regression and classification problems. For the classification problem, tag encoding uses unique hot code. If the label of the input sample x_i is $y_i = (y_{i1}, y_{i2}, \ldots, y_{iQ}) \in R^Q$, the unique hot code [0,0,1…,0] indicates that the input sample is of the third type. All labels can be represented as

$$Y = (y_1, y_2, \ldots, y_i, \ldots, y_N)^T \tag{3}$$

In Eq. (3), Q is the number of categories and Y is the label matrix. After input sample X passes through the BLN, the following output matrix is obtained:

$$\hat{Y} = (\hat{y}_1, \hat{y}_2, \ldots, \hat{y}_i, \ldots, \hat{y}_N)^T \tag{4}$$

E. MODELING AND RESOLVING FOR BLN

Based on the previous discussion, in BLN, only the weight matrix requires training, which undoubtedly greatly reduces the training amount of the BLN. BLN training is based on the following objective functions:

$$\arg\min_{W^m}(||Y - \hat{Y}||_2^2 + \frac{\lambda}{2}||W^m||_2^2) \tag{5}$$

In Eq. (5), $||Y - \hat{Y}||_2^2$ represents the training error, which is minimized by the training process. $\frac{\lambda}{2}||W^m||_2^2$ is the regularization term that is used to prevent over-fitting of the model, where λ is the regularization coefficient with a value range of 0-1.

IV. IMPROVEMENT OF BLN INCREMENTAL LEARNING AND STRUCTURE SIMPLIFICATION

Incremental learning means that when there are new samples, the model only needs to perform incremental training or local updates based on new data. This training method can make the model update faster, and the cost of the model update is smaller. Literature [29] proposed a dynamic updating neural network training algorithm was proposed. By obtaining a pseudo-matrix [30], this algorithm provides a fast update method for connection weights when new input data are available. Since then, incremental learning has been applied to machine learning algorithms such as random forest [31] and SVM [32], gradually becoming an important learning method in the field of machine learning. In this study, two incremental learning algorithms, the Enhanced Node Increment algorithm (EIBLS) and the input data increment algorithm (IIBLS), are used to improve the classification accuracy of the traditional BLN model.

A. ENHANCED NODE INCREMENT ALGORITHM OF BLN (EIBLN)

The enhanced node incremental learning algorithm is a learning algorithm that keeps the number of feature nodes unchanged in the network and increases the number of enhanced nodes to improve the feature extraction ability of the model. Its structure is shown in Fig. 2.

When several enhancement nodes are added to the model, the hidden layer matrix of the model is expanded from $A = [Z^n|H^m]$ to $A^{m+1} = [A|\xi(Z^n W_{m+1} + \beta_{m+1})]$, where W_{m+1} and β_{m+1} are the newly added weight matrix and bias matrix, respectively, and ξ is the activation function. Using a pseudo-fitting operation, the pseudo-fitting matrix of the hidden layer matrix is

$$(A^{m+1})^+ = \begin{bmatrix} A^+ - DB^T \\ B^T \end{bmatrix} \tag{6}$$

where $D = A^+\xi(Z^n W_{h_{m+1}} + \beta_{h_{m+1}})$

$$B^T = \begin{cases} C^+ & C \neq 0 \\ (1 + D^T D)^{-1} B^T A^+ & C = 0 \end{cases} \tag{7}$$

and $C = \xi(Z^n W_{h_{m+1}} + \beta_{h_{m+1}}) - AD$, C^+ is the pseudo inverse of C.

According to Eq.(6) and Eq.(7), the connection weight W^{m+1} of the hidden and output layers is updated as follows.

$$W^{m+1} = \begin{bmatrix} W^m - DB^T Y \\ B^T Y \end{bmatrix} \tag{8}$$

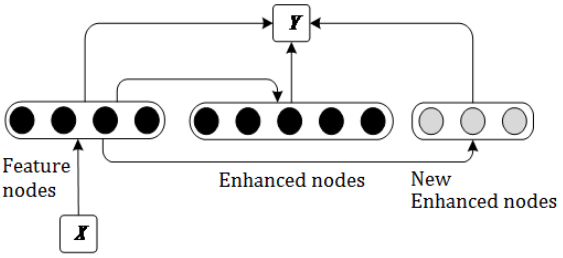

FIGURE 2. Enhanced node incremental algorithm of BLN.

B. INPUT DATA INCREMENT ALGORITHM OF BLN (IIBLN)

In the era of big data, the amount of data is growing rapidly, which requires machine learning models to be updated or constructed rapidly. Traditional deep learning models usually need to be retrained when the input data increases, which is time-consuming and laborious. Broad learning networks have a special advantage in dealing with this problem: they may use an input data increment algorithm to update themselves quickly.

As shown in Fig. 3, we assume that the newly added data to the BLN are X_a. A_n^m is the original hidden layer matrix, including the n groups of feature mappings and the m groups of enhanced mappings. Owing to the new data, the hidden layer is updated to

$$A_x = [\varphi(X_a W_{e1} + \beta_{e1}), \ldots, \varphi(X_a W_{en} + \beta_{en})| \\ \xi(Z_x^n W_{h1} + \beta_{h1}), \ldots, \xi(Z_x^n W_{h_m} + \beta_{h_m})] \quad (9)$$

In Eq. (9), $Z_x^n = [\varphi(X_a W_{e_1} + \beta_{e_1}), \ldots, \varphi(X_a W_{e_n} + \beta_{e_n})]$ is the updated part of the original feature nodes and W_{e_i}, W_{hj}, β_{e_i}, β_{h_j} is a randomly generated matrix. After updating, the hidden layer matrix is

$${}^x A_n^m = \begin{bmatrix} A_n^m \\ A_x^T \end{bmatrix} \quad (10)$$

The corresponding pseudo-inverse operation is:

$$({}^x A_n^m)^+ = [(A_n^m)^+ - BD^T | B] \quad (11)$$

where $D^T = A_x^T (A_n^m)^+$

$$B^T = \begin{cases} C^+ & C \neq 0 \\ (1 + D^T D)^{-1} (A_n^m)^+ D & C = 0 \end{cases}$$
$$C = A_x^T - D^T A_n^m, \quad (12)$$

Finally, the weight ${}^x W_n^m$ is updated to:

$${}^x W_n^m = W_n^m + (Y_a^T - A_x^T W_n^m) B \quad (13)$$

In Eq. (13), Y_a^T is the label corresponding to the new data X_a.

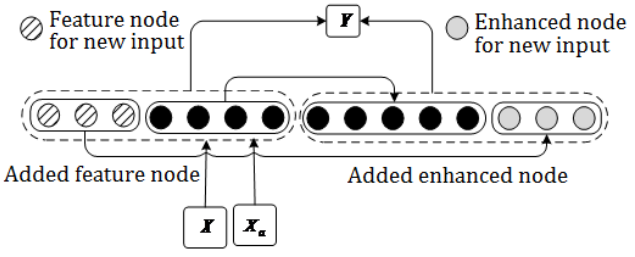

FIGURE 3. Input data increment algorithm of BLN.

C. THE IMPLEMENTATION OF BLN

According to the above improvements to BLN, the overall implementation process of the BLN Incremental model including feature-mapping nodes, enhancement nodes, and new inputs is shown in Algorithm 1.

Algorithm 1 The Implementation of the Incremental Learning of BLN

Input: training set X;
Output: W
for $i = 0; i \leq n$ do
  Random W_{ei}, β_{ei};
  Calculate $Z_i = [\phi(XW_{ei} + \beta_{ei})]$;
end
Set feature mapping group $Z^n = [Z_1, \ldots, Z_n]$;
for $j = 1; j \leq m$ do
  Random W_{hj},β_{hj};
  Calculate $H_j = [\xi(Z^n W_{hj} + \beta_{hj})]$;
end
Set enhancement nodes group $H^m = [H_1, \ldots, H_m]$;
Set A_n^m and calculate A_n^{m+1};
While *loss function does not converge* do
 if p *enhancement nodes are added* then
  Random W_{hm+1},β_{hm+1};
  Calculate $H_{m+1} = [\xi(Z^n W_{hm+1} + \beta_{hm+1})]$;
  Update A_n^{m+1};
  Calculate $(A_n^{m+1})^+$ and W_n^{m+1};
  $m = m + 1$;
 else
  if $n + 1$ *feature mapping is added* then
   Random $W_{e_{n+1}}$, $\beta_{e_{n+1}}$;
   Calculate $Z_{n+1} = [\phi(XW_{e_{n+1}} + \beta_{e_{n+1}})]$;
   Random W_{ex_i}, β_{ex_i}, $i = 1, \ldots, m$;
   Calculate $H_{ex_{n+1}} = [\xi(Z_{n+1} W_{ex_i} + \beta_{ex_i}), \ldots, \xi(Z_{n+1} W_{ex_m} + \beta_{ex_m})]$;
   Update A_{n+1}^m;
   Update $(A_{n+1}^m)^+$ and W_{n+1}^m;
   $n = n + 1$;
  else
   New inputs are added as X_a;
   Calculate A_x;
   Update $({}^x(A_n^m)^+$ and $({}^x W_n^m)$;
  end
 end
end
Set W;

Notice that all the pseudo inverse of the involved matrix are calculated by the regularization approach. Specifically, this algorithm only needs to compute the pseudo inverse of the additional enhancement nodes instead of computations of the entire (Am+1) and thus results in fast incremental learning.

D. STRUCTURE SIMPLIFICATION

After the broad expansion with added mapped features and enhancement nodes via incremental learning, the structure may have a risk of being redundant due to poor initialization or redundancy in the input data. Generally, the structure can be simplified by a series of low-rank approximation methods. In this paper, we adopt the classical SVD as a conservative choice to offer structure simplification for the proposed broad model. The simplification can be done in different ways: 1) during the generation of mapped features; 2) during the generation of enhancement nodes; or 3) in the completion of broad learning. After comparison, we choose to simplify the model in the completion of broad learning.

V. STORED-GRAIN SITUATION RISK PREDICTION MODEL BASED ON BLN

The framework of the stored-grain situation risk-prediction model based on the improved BLN is shown in Fig. 4. Stored-grain status data are usually in the form of temperature, humidity, gas composition, insect condition, etc., which present multi-modal characteristics. Integrating information from multiple modes is necessary for building models using machine learning. However, existing broad learning networks and their improved algorithms only use single-mode data when classifying or predicting patterns. Based on the above-improved framework of the broad learning network, this study combined the multi-modal characteristics of the stored-grain situation data and proposed the following risk-prediction model, as shown in Fig. 4. The model aims to improve prediction accuracy by learning and fusing data from multiple modes.

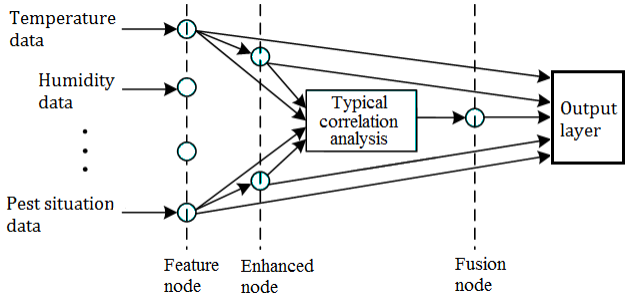

FIGURE 4. The framework of warehouse grain situation risk prediction model.

As shown in Fig. 4, a typical correlation analysis (CCA) module and feature fusion nodes are added to the proposed stored-grain situation risk prediction model based on a broad learning network. First, feature extraction of the stored-grain situation data with various modes is carried out, and the extracted features are input into the correlation analysis module for correlation learning. Feature fusion is carried out in the feature fusion node, and finally, pattern classification is realized through the output layer. The advantage of this model is that, compared with the classification model using a single mode, it can obtain a higher classification performance by making full use of the fusion features of multiple modes.

Canonical correlation analysis can be used for dimensionality reduction of multiple datasets. It can map multiple datasets with different modes to the same data space, according to an association rule. The CAA can be fused and mapped in a cascading manner, and its mathematical definition is as follows:

Assuming that $X = \{x_1, x_2, \cdots, x_n\}$ and $Y = \{y_1, y_2, \cdots, y_n\}$ are two n-dimensional datasets, a new coordinate space is obtained through transformation via basis vectors u and v, respectively. The correlation parameters of datasets X and Y are defined as:

$$\rho = \max_{u,v} \frac{u^T \sum_{xy} v}{\sqrt{u^T \sum_{xx} u} \sqrt{v^T \sum_{yy} v}} \tag{14}$$

In the above equation, $\sum_{xy}$, $\sum_{xx}$, and $\sum_{yy}$ are interclass and intraclass covariance matrices, respectively.

$$\begin{aligned} \sum_{xy} &= E\left[xy^T\right] = \frac{1}{n}\sum_{i=1}^{n} x_i y_i^T \\ \sum_{xx} &= E\left[xx^T\right] = \frac{1}{n}\sum_{i=1}^{n} x_i x_i^T \\ \sum_{yy} &= E\left[yy^T\right] = \frac{1}{n}\sum_{i=1}^{n} y_i y_i^T \end{aligned} \tag{15}$$

The correlation calculation in the above equation is an optimization problem, which can be transformed into a problem of solving eigenvalues.

It is assumed that the input data of the model have two modes: the number of samples is N, and the number of feature nodes and enhanced nodes are N1 and N2, respectively. The characteristic expression of one mode of data is $X_1 = [Z_1|H_1]$, which is generated by a broad learning unit, and its feature nodes and enhanced nodes can be expressed as $Z_1 = \left\{z_i|z_i \in R^{N_1}\right\}_{i=1}^{N}$ and $H_1 = \left\{h_j|h_j \in R^{N1}\right\}_{j=1}^{N}$ respectively; similarly, the feature expressions, feature nodes, and enhancement nodes of another modal data can be represented as $X_2 = [Z_2|H_2]$, $Z_2 = \left\{z_i|z_i \in R^{N2}\right\}_{i=1}^{N}$, and $H_2 = \left\{h_j|h_j \in R^{N_2}\right\}_{j=1}^{N}$, respectively, generated by another broad learning unit. To better learn the common characteristics of the two modal datasets, they are first mixed and then input into the fusion node layer. In this study, considering the convenience of processing, the data of the two modes are simply connected in parallel as the total feature that is extracted last and the net input of the fusion node, namely:

$$F^{N\times 2(N_1+N_2)} = \left[X_1^{N\times(N_1+N_2)}|X_2^{N\times(N_1+N_2)}\right] \tag{16}$$

Here, F represents the new input of the fusion node layer. To better fuse the data of different modes, this study introduces a fusion node mapping layer. The features of the different modes are abstractly fused by referring to the nonlinear fitting of a traditional neural network. Finally, the output matrix is used for feature learning to improve the classification performance of the model. Assuming that the number of nodes in the fusion layer is N3, the output of the fusion node layer is.

$$T^{N\times N_3} = \phi\left(F^{N\times 2(N_1+N_2)} \cdot W_t^{2(N_1+N_2)\times N_3} + b_t^N \times N_3\right) \tag{17}$$

where $\phi(\cdot)$ is an S-type nonlinear activation function.

VI. EXPERIMENTAL RESULTS AND ANALYSIS

A. DATA ACQUISITION AND PROCESSING

The experimental data are the 2019-2020 stored-grain situation measurement and control data from a national granary in China. This granary is equipped with a full set of stored-grain situation measurement and control systems that can measure

the temperature, humidity, worm situation, and gas composition. The measurement and control software can dynamically display the cloud and trend maps of the temperature and humidity in the granary visually. In this study, 735 pieces of temperature and humidity data (in the form of Excel tables, each of which included one item of average temperature in the granary, one item of average temperature in each layer of the grain pile, 12 items of maximum and minimum temperature, one item of humidity in the granary, and one item of temperature and humidity outside the granary), 105 pieces of stored-grain situation reports (in the form of Word files), 76 cloud map images of temperature and humidity (JPG image format file), 20 insect situation reports (Word format file), 24 insect density maps (JPG image format file), and 10 gas composition reports (Word file), were obtained for the experiments.

There are two types of data (text and image data) with multiple modes (each mode corresponds to a data source). First, we preprocessed the text data as follows: exported the data in Word files and Excel files, removed the sick data, and formed four plain text files of temperature, humidity, insect pests, and gas components with a total of 23,275 data points, where 70% of the data were taken as training sets and labeled. SamplePairing tool was then used to expand the image data to 600 pieces, and the Labelimg tool was used to add labels.

This study divides the data into two groups according to the year: text data and image data, which are composed of multiple modal data. The proposed model takes the multi-modal data as the input of the broad learning network, and via the typical correlation analysis module shown in Fig. 4, the stored-grain situation risk characteristics are extracted at a deeper level to improve the accuracy of the prediction. In the experiment of text data, the model was trained with the text stored-grain situation data of 2019-2020 as the training set. The temperature, humidity, and pest situation data of a day are taken as a model vector, and 720 model vectors were used in total. The data was sampled once a day, and the data that was not sampled on time was processed by the interpolation method. All data were batch normalized before being used for model training. In the experiment of image data,

In the stored-grain situation risk forecast dataset, the normal data account for the majority; therefore, it is a typical unbalanced dataset. To improve the proportion of risk data and ensure the balance between the data of various risk types, we adopted COMSOL Multiphysics software to simulate the ecological environment of the granary. COMSOL Multiphysics has efficient computing power and unique multi-field fully coupled analysis ability, which can ensure the high precision of the numerical simulation. Firstly, the heat transfer module and porous media flow module are called in COMSOL Multiphysics software to establish a set of simulation modeling methods for multi-physical field coupling analysis. The Navie-Stokes (NS) equation is used to construct the multi-field coupling mathematical model of temperature, humidity, and micro airflow, and the coupling simulation is carried out for each initial physical field of the grain pile. The multi-mode simulation data changed with time is generated and visualized to make up for the deficiency of image data. By changing the initial conditions of the simulation model and artificially setting the simulation parameters, we deduced the low-, medium-, and high-risk conditions and obtained a large number of minority types of data, which were added to the training dataset to ensure the balance of data types in the dataset. Finally, we split the data into training and test sets in a 7:3 ratio.

In addition, the data were preprocessed before being used for model training. For the general methods of signal processing, Literature [33] addresses the role of emerging technologies and mathematical tools in integrating computational intelligence and digital signal processing in education and has a great inspiration for our research on signal preprocessing. In our study of signal preprocessing, first, the text data was cleaned according to the big data cleaning process, then for the image data, the median filtering method was used to filter the salt and pepper noise that is from abnormal sensors. Finally, normal distribution normalization is used for batch normalization of data to accelerate the convergence of the model.

B. CLASSIFICATION OF RISK LEVELS AND INDEX OF EVALUATION

According to the actual grain storage experience, we divide the storage risk of grain into the following grades, as shown in the label. It should be noted that the risk level of the stored-grain situation given in Table 1 has limitations. For example, the temperature of the grains stored in the granary in summer may be higher than the normal index. In this case, we labeled some samples in the dataset using manual analysis and judgment.

TABLE 1. Risk grading of stored-grain situation.

Level	Explanation
Normal	Stored-grain situation indicators are in the normal range, without intervention
Low risk	Individual indicators of stored-grain conditions are abnormal, but deviate little from normal, which requires close attention
Medium risk	Several indicators of a stored-grain situation are abnormal or some indicators deviate from the normal value, further monitoring and evaluation and intervention should be carried out if necessary
High risk	Many indicators of the stored-grain situation deviate greatly from the normal, and the situation is in a dangerous state, which requires immediate intervention

Using accuracy as the evaluation index of the classifier is unfair to unbalanced data. To objectively evaluate the performance of classification algorithms, researchers often evaluate the algorithm performance according to the concept introduced using a confusion matrix. According to the confusion matrix in Table 2, indices such as Recall, Precision, F-value, and G-mean are introduced to evaluate the performance of the model in this study.

TABLE 2. Confusion matrix.

		Prediction	
		Positive	Negative
Reference	Positive	TP	FN
	Negative	FP	TN

Some indicators are defined as follows:

$$R = \frac{TP}{TP + FN}$$
$$P = \frac{TP}{TP + FP}$$
$$F - value = \frac{2RP}{R + P}$$
$$G{-}mean = \sqrt{\frac{TP}{TP + FN} \times \frac{TN}{TN + FP}} \tag{18}$$

In the above equation, P is the precision rate, R is the recall rate, F-value is the weighted average of the recall rate and precision rate, and G-mean is the comprehensive index of positive case accuracy and negative case accuracy.

To compare the robustness of some models in the literature, a simplified robustness evaluation method based on random sampling is proposed to evaluate the robustness of the model against the influence of input disturbance. In this paper, based on the loss function as the model optimization basis, all possible value ranges of input variables are called global space, and the space composed of preset variation ranges of input variables for a certain satisfactory model is called the robustness space of the model, and its robustness index F_m is defined as

$$F_m = 1 - \frac{\Delta f_m}{\Delta f} \tag{19}$$

where Δf_m is the difference between the maximum value and the minimum value of the loss function f that is sampled in the robust space of model m; Δf is the difference between the maximum value and the minimum value of the loss function f that is sampled in the global space. The larger the robustness index F_m is, the better the anti-input disturbance performance (robustness) of the model m is reflected. When the robustness index F_m is greater than the threshold set according to the actual needs, the model m can be considered to meet the requirements of robustness.

C. EXPERIMENTAL SETTINGS

The purpose of the experiment is to test whether the broad learning model proposed in this paper can be used as an alternative to deep learning to ensure prediction accuracy and whether it is better than the existing stored-grain situation prediction model. Therefore, this study is compared with some deep learning methods, mainly in terms of the recognition rate, training and testing time, as well as the sensitivity of parameters, and compared with other stored-grain situation prediction models.

In the experiment, we compared the basic broad learning network (BLN), the broad learning of Cascade Feature Mapping (CFBLS) [13], and the broad learning of finite connection cascade feature mapping (LCFBLS) [13]. CFBLS improves the connection mode of the feature nodes in the broad learning model and adopts a cascading connection structure. LCFBLS is similar in structure to CFBLS, but the last set of feature nodes is used to generate enhancement nodes. Meanwhile, the incremental broad learning method in this study was compared with four deep learning methods: the BERT model [34], the transformer network model [35], the SSD model [36], and YOLOv5 [37].

The loss function used for model training in this study is the cross-entropy loss, as shown in Eq.(20), where q_i is 1 when sample i corresponds to the real label y otherwise, qi is 0.

$$Loss_{cross} = \frac{1}{N}\sum_{i=1}^{N} -q_i \log(p_i) \tag{20}$$

However, to avoid the overfitting problem of the model or the influence of inaccurate labels, this study introduced the label smoothing strategy [38] when calculating the cross-entropy loss. In this strategy, the possibility that the predicted samples belong to another category is also included in the measurement range, and the value qi in the cross-entropy loss is modified as shown in Eq. (21).

$$q_i = \begin{cases} 1 - \varepsilon(N-1)/N, & i = y \\ \varepsilon/N, & i \neq y \end{cases} \tag{21}$$

To verify the performance of the proposed algorithm on a small sample dataset, the initial training data of the experiment are only 1000, and then the samples are increased by 1000 each time to evaluate the impact of the incremental learning algorithm of broad learning on the accuracy of the model. The initial parameters of the broad learning network are set to 10×10 feature nodes and 100 enhancement nodes. In the incremental broad learning algorithm, the enhanced nodes are updated five times, and 100 enhanced nodes are added each time. The experiments are divided into two groups. Text and image data are used to evaluate the incremental learning algorithm of the proposed risk prediction model. Finally, the prediction performance of the proposed model based on correlation analysis is compared with that of other existing models.

The experimental environment is as follows: Intel Xeon E5 v3 processor, 32 GB memory, and NVIDIA GeForce RTX 2080 Ti 11GB graphics card. We used the CUDA 10.0 architecture, PyTorch deep learning framework, and Python3.6 programming language.

In our proposed BLN, the regularization parameter λ for ridge regression is set as 10^{-8}, meanwhile, the one= layer linear feature mapping with one-step fine-tuning to emphasize the selected features is adopted. In addition, the associated parameters W_{ei} and β_{ei}, for i=1,..., n are drawn from the standard uniform distributions on the interval $[-1, 1]$. For the enhancement nodes, the sigmoid function is chosen to establish BLN. For deep learning networks used for comparison,

TABLE 3. The results of Eibln.

Feature nodes	Input data	Enhancement node	F1-value	G-mean	Training time/s	Testing time/s
10×10	1000	100	0.83	0.88	8.84	0.12
10×10	1000	200	0.84	0.89	9.23	0.12
10×10	1000	300	0.85	0.90	11.34	0.13
10×10	1000	400	0.85	0.90	13.78	0.13
10×10	1000	500	0.87	0.91	15.72	0.14
10×10	1000	600	0.88	0.91	16.48	0.15

TABLE 4. The results of IIBLN.

Feature nodes	Input data	Enhancement node	F1-value	G-mean	Training time/s	Testing time/s
10×10	1000	100	0.83	0.88	8.84	0.12
10×10	2000	200	0.88	0.93	10.46	0.12
10×10	3000	300	0.91	0.94	22.51	0.13
10×10	4000	400	0.91	0.94	31.49	0.13
10×10	5000	500	0.94	0.96	45.43	0.14
10×10	6000	600	0.97	0.98	48.51	0.15

the hyper-parameters are tuned based on the back propagation, and its specific Settings are shown in the experiments below.

D. RESULTS AND ANALYSIS

The model in this paper can be used for both classification and prediction. Basic BLNS are available for classification. BLN that is introduced incremental learning can be used for prediction because it covers the time-sequential characteristics of the context. In the experiment, the first set of data is essentially a time series, which we used to do the prediction experiment, and compared with BERT, Transformer, and other common prediction models. In the experiment of the second set of data, we only did the classification experiment and compared it with some popular CNN networks. Note that the model's predictions are also logical, not numerical. Real results are obtained by manual labeling.

1) THE FIRST GROUP OF EXPERIMENTS

To verify the effectiveness of the proposed incremental broad learning model for stored-grain situation risk prediction, we first used text data to build a model according to the method proposed above and compared the prediction accuracy of the models using the EIBLS incremental learning algorithm and IIBLS incremental learning algorithm. The textual data used in the experiment included temperature, humidity, and bug data, which are derived from EXCEL files. After the text data was preprocessed, it is numerically and normalized to form 720 model vectors of temperature, humidity, and insect condition, which are used as model input vectors. The results of model training are shown in Fig. 5. It can be seen that with the increase in the number of training rounds, the loss curve in the incremental learning mode declines and converges faster. The results are presented in Table 3 and Table 4, respectively.

As can be seen from Table 3 and Table 4, with the introduction of incremental learning into broad learning, the prediction accuracy of the model gradually improved. Because the IIBLS can provide new information for the prediction model, under the condition of the same incremental nodes, it has better prediction accuracy than the algorithm that only adds enhanced nodes. For example, under the condition that the number of enhanced nodes is 600, the prediction accuracy of the IIBLS model with input data is approximately 10% higher than that of EIBLS with 1000 input data. But at the same time, the increase of input data leads to the increase of data processing overhead, which makes the training time of the IIBLS model longer than that of EIBLS under the same enhancement nodes.

Next, we compared the results of the proposed broad learning model with the basic broad learning model, other improved broad learning models, and two types of deep learning models (BERT and Transformer) in terms of prediction accuracy and model training time. The key structural parameters of the BERT model are consistent with Google's official pre-trained model, and the Settings are as follows: the number of hidden layers is set to 12, and the number of taps in the multi-tap self-attention mechanism is set to 8. Adam optimizer is used. For the transformer, the number of layers is set to 4, and the number of self-attention heads is set to 8. The relative position-coding length is 8, the batch size is 32, and a ranger optimizer with an initial learning rate of 0.0004 is used during the training. The learning rate of each epoch is decayed to 0.8 times the original, and the maximum iteration times in the training process are set to 30. Beam search is used during decoding, and the cluster size is set to 3. The amount of training data is increased from 1000 to 6000, and the comparison results are listed in Fig. 6.

As shown in Fig. 6, the model proposed in this study is superior to the basic broad learning model and the two improved broad learning models in terms of the prediction accuracy rate and training time. In particular, the training time of the proposed model is significantly reduced because of the incremental learning algorithm. Compared with the two

TABLE 5. The results of EIBLS.

Feature node	Input data	Enhancement node	F1-value	G-mean	Training time/s	Testing time/s
10×10	100	100	0.78	0.81	27.53	0.33
10×10	100	200	0.79	0.82	29.38	0.33
10×10	100	300	0.81	0.83	32.74	0.34
10×10	100	400	0.81	0.83	34.67	0.35
10×10	100	500	0.83	0.85	35.14	0.35
10×10	100	600	0.84	0.86	37.65	0.36

TABLE 6. The results of IIBLS.

Feature node	Input data	Enhancement node	F1-value	G-mean	Training time/s	Testing time/s
10×10	100	100	0.78	0.81	27.53	0.33
10×10	200	200	0.83	0.85	34.55	0.33
10×10	300	300	0.88	0.92	52.78	0.34
10×10	400	400	0.91	0.95	63.22	0.34
10×10	500	500	0.94	0.96	70.67	0.36
10×10	600	600	0.96	0.98	79.15	0.36

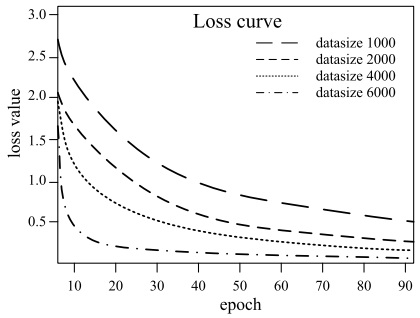

FIGURE 5. Loss cure for the first group of experiments.

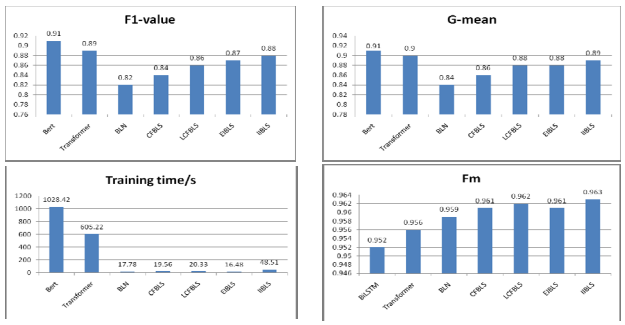

FIGURE 6. Comparison between the proposed model and the other models on the first dataset.

common deep learning algorithms, IIBLS is very close to the prediction accuracy of the two deep learning methods, and EIBLS has only a small gap. However, the training time of the two broad learning models in this study is much shorter than that of the two deep learning models. The accuracy of the improved BLN is about 2.3% higher than that of the traditional BLN, and the training time is about 20 times shorter. In addition, it can also be seen from Fig. 6 that the robustness of the BLN model is better than that of the deep learning, because the multi-layer structure of deep learning model has the effect of amplifying disturbance, while BLN does not. It can be seen that the proposed broad learning models can be used as a substitute for the deep learning models for the prediction of the situation risk of stored grain.

2) THE SECOND GROUP OF EXPERIMENTS

In this experiment, we used image data to model the problem of stored-grain situation risk prediction and compared the prediction accuracy of models using the EIBLS and IIBLS incremental learning algorithms. All images are adjusted to a resolution of 224 × 224. The perceptual domain of the basic broad learning network is 4 × 4, and the feature map and pool size are both 3. The training loss curve of the model is shown in Fig. 7. As shown in Fig. 7, we obtained training results consistent with numerical data for image data. The comparison results are presented in Table 5 and Table 6 respectively.

As can be seen from Table 5 and Table 6, for image data, with the introduction of incremental learning, the prediction accuracy of the models improves faster. The IIBLS incremental learning algorithm had higher prediction accuracy than the EIBLS incremental learning algorithm under the same condition of incremental nodes. However, owing to the time cost of image processing, the training time of the models is slightly longer than that of the text input data.

To verify the effectiveness of the BLN prediction model with incremental learning for image data, the EIBLS and IIBLS prediction models are compared with the basic BLN, CFBLS, LCFBLS, and two deep neural network image detection models called SSD and YOLOv5 in terms of prediction performance. The comparison results are presented in Fig. 8. The parameters of each comparison model are set as follows: the initial structure of the IIBLS is set as a 4 × 4 awareness domain, 100 enhancement nodes, and 10 × 10 feature nodes, and the feature mapping and pool size is 3. The initial structures of the BLN, CFBLS, and LCFBLS are set to 1000 enhancement nodes and 100 × 10 feature nodes.

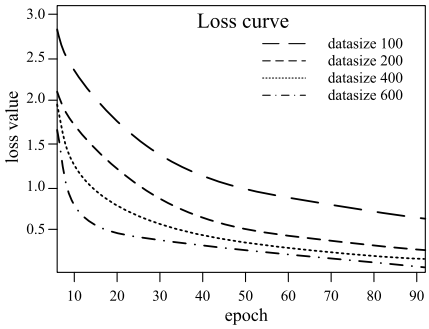

FIGURE 7. Loss cure for the second group of experiments.

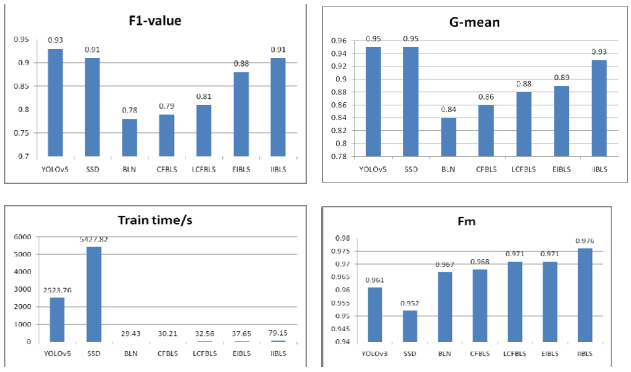

FIGURE 8. Comparison between the proposed models and the other models on the second dataset.

As can be seen from Fig. 8, the method proposed in this study is superior to the basic broad learning model and the two improved broad learning models in terms of the accuracy rate of prediction and training time for image data. Compared with the two common deep learning network models for one-stage object detection, IIBLS and EIBLS have only a small gap, but the training time is much shorter than that of the two typical deep learning models. For Fm (Robustness, see Eq. (19)) index, similar results are also obtained with the first set of data. The accuracy of the improved BLN is about 14.4% higher than that of the traditional BLN, and the training time is about 30 times shorter. It can be seen that the broad learning model proposed in this study can be used as a substitute for the deep learning model for the prediction of stored-grain situation risk, regardless of whether the data are text or image.

3) ABLATION EXPERIMENT

Previously, we discussed the prediction performance of the BLN combined with an incremental learning algorithm for different types of datasets, from which we can see the advantages of our proposed method for the prediction of stored-grain situation risk. Next, we further discuss the predictive performance of the BLN model after the introduction of the CCA module through ablation experiments. The CCA module fuses features from different types of data. The introduction of the CCA module makes full use of the complementarity of different types of features and further improves the prediction performance of the model. The results of the ablation experiments are listed in Table 7.

TABLE 7. Ablation experiment.

Basic BLN	EIBLS	IIBLS	CCA	F1-value	G-mean
√	√			0.87	0.88
√		√		0.88	0.91
√	√	√		0.90	0.92
√	√		√	0.91	0.93
√		√	√	0.94	0.95
√	√	√	√	0.97	0.98

As shown in Table 7, the prediction performance of the model is further improved after the introduction of the CCA module.

4) COMPARE RESULTS WITH SOME OF THE PREVIOUS STUDIES

To further clarify the effectiveness and advancement of our model, we compared it with the four models discussed in the related works section in terms of performance, and the comparison results are shown in Table 8.

TABLE 8. The comparison between our model and the previous studies.

Model Name	Accuracy	Complexity	Robustness	Forecast duration	The difficulty of training
Empirical model	Low	Low	Poor	-	-
Three-transfer model [19]	Medium	Medium	Average	Short time	-
Machine learning model [8,23,24]	Medium	Medium	Average	Short time	Easy
Deep learning model [25,26,27]	High	High	Good	Long time	Difficult
Our model	High	Medium	Excellent	More time	Moderate difficulty

It can be seen from Table 8, for the risk prediction of grain storage, the model proposed in this paper is superior to the existing models in terms of comprehensive performance.

VII. CONCLUSION

Based on the broad learning idea that has been proposed in recent years, this study introduces incremental learning and correlation analysis in the improved broad learning network proposed in this study to establish a risk point prediction model for stored-grain situations. It is found that the incremental learning training method can make the prediction accuracy of the model close to the deep learning model. The experimental results show that compared with traditional BLNS, the precision of grain situation risk prediction can be improved by more than 10%. Compared with deep learning, the training time is reduced by more than 50% under the condition that the prediction accuracy does not decrease, Moreover, it can accurately predict the changes of storage grain conditions within one month, and the prediction time is longer than some existing deep learning models. Aiming at

the problems of deep learning models, such as long training time and large resource demand, this model significantly reduces the training difficulty and resource consumption under the premise that the prediction accuracy does not decrease. Although the accuracy of this model is not comparable to that of the deep learning model, its fast ''incremental training'' features make it have better application prospects in fields with low accuracy requirements and large data changes, Such as weather forecasting, air pollution, infectious disease forecasting and so on. At present, as an alternative to the prediction model based on deep learning, the broad learning prediction model proposed in this study still has the following limitations: (1)The precision of target recognition is low due to the inability of broad learning to extract the deep features of sequences;(2) There may be a large number of redundancies in the network structure, resulting in reduced efficiency of the model;(3) There are still few new technologies related to model improvement. Future work will focus on improving the fusion effect of grain situation data with different modes and how to introduce the attention mechanism into broad learning to further improve the prediction accuracy and application range of the broad learning model.

ACKNOWLEDGMENT

The authors would like to thank the colleagues and students who participated in the research activities. Their works help to improve the ideas and results presented in this article.

REFERENCES

[1] J. Yuan, D. Zheng, X. Meng, and H. Zhao, ''Research progress of grain monitoring and early warning technology,'' *J. Chin. Cereals Oils Assoc.*, vol. 37, no. 11, pp. 19–26, Mar. 2022. [Online]. Available: https://kns.cnki.net/kcms/detail/11.2864.ts.20220302.1635.004.html

[2] C.-H. Wu, J.-M. Ho, and D. T. Lee, ''Travel-time prediction with support vector regression,'' *IEEE Trans. Intell. Transp. Syst.*, vol. 5, no. 4, pp. 276–281, Dec. 2004.

[3] N. M. Abdulkareem and A. M. Abdulazeez, ''Machine learning classification based on Radom forest algorithm: A review,'' *Int. J. Sci. Bus.*, vol. 5, no. 2, pp. 128–142, 2021.

[4] J. Contreras, R. Espinola, F. J. Nogales, and A. J. Conejo, ''ARIMA models to predict next-day electricity prices,'' *IEEE Trans. Power Syst.*, vol. 18, no. 3, pp. 1014–1020, Aug. 2003.

[5] Y. Wang, ''Predicting stock price using fuzzy grey prediction system,'' *Exp. Syst. Appl.*, vol. 22, no. 1, pp. 33–38, Jan. 2002.

[6] Z. Xiao, S.-J. Ye, B. Zhong, and C.-X. Sun, ''BP neural network with rough set for short term load forecasting,'' *Exp. Syst. Appl.*, vol. 36, no. 1, pp. 273–279, Jan. 2009.

[7] Z. Li, ''Prediction of grain storage temperature based on deep learning,'' *Revista de la Facultad de Ingeniería*, vol. 32, no. 14, pp. 918–924, 2017.

[8] S. Duan, W. Yang, X. Wang, S. Mao, and Y. Zhang, ''Forecasting of grain pile temperature from meteorological factors using machine learning,'' *IEEE Access*, vol. 7, pp. 130721–130733, 2019.

[9] C. L. P. Chen and Z. Liu, ''Broad learning system: An effective and efficient incremental learning system without the need for deep architecture,'' *IEEE Trans. Neural Netw. Learn. Syst.*, vol. 29, no. 1, pp. 10–24, Jan. 2018.

[10] C. L. P. Chen and Z. Liu, ''Broad learning system: A new learning paradigm and system without going deep,'' in *Proc. 32nd Youth Academic Annu. Conf. Chin. Assoc. Autom. (YAC)*, May 2017, pp. 1271–1276.

[11] C. L. P. Chen, Z. Liu, and S. Feng, ''Universal approximation capability of broad learning system and its structural variations,'' *IEEE Trans. Neural Netw. Learn. Syst.*, vol. 30, no. 4, pp. 1191–1204, Apr. 2019.

[12] C. Ren, C. Yuan, Y. Sun, Z. Liu, and J. Chen, ''Research of broad learning system,'' (in Chinese), *Appl. Res. Comput.*, vol. 38, no. 8, pp. 2258–2267. Aug. 2021.

[13] Z. Wang, X. Xu, H. Liu, and F. Sun, ''Cascade broad learning for multimodal material recognition,'' (in Chinese), *Trans. Intell. Syst.*, vol. 15, no. 4, pp. 787–794. Jul. 2020.

[14] R. Ye, Q. Kong, D. Li, Y. Chen, Y. Zhang, and C. Liu, ''Shrimp freshness detection method based on broad learning system,'' (in Chinese), *Spectrosc. Spectral Anal.*, vol. 42, no. 1, pp. 164–169, Jan. 2022.

[15] C. Jia, H. Liu, X. Xu, and F. Sun, ''Multi-modal information fusion based on broad learning method,'' (in Chinese), *Trans. Intell. Syst.*, vol. 14, no. 1, pp. 150–157, Jan. 2019.

[16] T. Wu, Y. Zhuang, B. Fan, H. Guo, W. Fan, C. Yi, and K. Xu, ''Multidomain feature fusion for varying speed bearing diagnosis using broad learning system,'' *Shock Vibrat.*, vol. 2021, pp. 1–8, Jan. 2021.

[17] P. K. Wong, L. Yao, T. Yan, I. C. Choi, H. H. Yu, and Y. Hu, ''Broad learning system stacking with multi-scale attention for the diagnosis of gastric intestinal metaplasia,'' *Biomed. Signal Process. Control*, vol. 73, Mar. 2022, Art. no. 103476.

[18] J. H. Yuan, D. Zheng, X. X. Meng, and H. Y. Zhao, ''Research progress of grain monitoring and early warning technology,''(in Chinese), *J. Chin. Cereals Oils Assoc.*, vol. 37, no. 11, pp. 19–26, 2022.

[19] L. I. Quemada-Villagómez, F. I. Molina-Herrera, M. Carrera-Rodríguez, M. Calderón-Ramírez, G. M. Martínez-González, J. L. Navarrete-Bolaños, and H. Jiménez-Islas, ''Numerical study to predict temperature and moisture profiles in unventilated grain silos at prolonged time periods,'' *Int. J. Thermophys.*, vol. 41, no. 5, pp. 1–28, May 2020.

[20] R. Guangyue, L. Yanan, P. Wei, D. Xu, and Z. Ledao, ''Experimental and numerical research on squat silo and large size horizontal warehouse during quasi-steady-state storage,'' *Int. J. Agricult. Biol. Eng.*, vol. 9, no. 6, pp. 214–222, 2016.

[21] J. Yin, Z. D. Wu, and X. M. Wu, ''Analysis of temperature field recurrence in discrete points of grain heap based on coupling of temperature and humidity fields,'' (in Chinese), *J. Chin. Cereals Oils Assoc.*, vol. 29, no. 12, pp. 95–101, 2014.

[22] Z. Liu, Z. Wu, X. Wang, J. Song, and W. Wu, ''Numerical simulation and experimental study of deep bed corn drying based on water potential,'' *Math. Problems Eng.*, vol. 2015, pp. 1–13, Jan. 2015.

[23] Z. Li, Y. Zhu, T. Zhen, and C. Zhu, ''Research on grain storage temperature prediction model based on time series method,'' *IPPTA, Quart. J. Indian Pulp Paper Tech. Assoc.*, vol. 30, no. 4, pp. 99–100, 2018.

[24] Q. Wang, J. Feng, F. Han, W. Wu, and S. Gao, ''Analysis and prediction of grain temperature from air temperature to ensure the safety of grain storage,'' *Int. J. Food Properties*, vol. 23, no. 1, pp. 1200–1213, Jan. 2020.

[25] Y. Wu, H. Yang, K. Zhou, Y. Wang, and Y. Zhu, ''Application of bidirectional LSTM neural network in grain stack temperature prediction,'' in *Proc. 17th Int. Conf. Bio-Inspired Comput., Theories Appl.*, Wuhan, China, Dec. 2022, pp. 385–395.

[26] S. Duan, W. Yang, X. Wang, S. Mao, and Y. Zhang, ''Temperature forecasting for stored grain: A deep spatiotemporal attention approach,'' *IEEE Internet Things J.*, vol. 8, no. 23, pp. 17147–17160, Dec. 2021.

[27] H. C. Feng, ''Pre-warning model of stored grain safety risk based on temperature and humidity and its application,'' *Zhengzhou, Henan Univ. Technol.*, pp. 23–36, Jan. 2020.

[28] P. Raiguru, M. Sahani, S. K. Rout, D. C. Panda, and R. K. Mishra, ''A digital direction of arrival estimator based on fast on-line sequential random vector functional link network,'' *AEU-Int. J. Electron. Commun.*, vol. 142, Dec. 2021, Art. no. 153986.

[29] C. L. P. Chen and J. Z. Wan, ''A rapid learning and dynamic stepwise updating algorithm for flat neural networks and the application to time-series prediction,'' *IEEE Trans. Syst., Man Cybern., B*, vol. 29, no. 1, pp. 62–72, Feb. 1999.

[30] F. L. Tiplea and V.-F. Dragoi, ''Generalized inverse based decoding,'' in *Proc. IEEE Int. Symp. Inf. Theory (ISIT)*, Jun. 2022, pp. 2791–2796.

[31] A. Wang, G. Wan, Z. Cheng, and S. Li, ''Incremental learning extremely random forest classifier for online learning,'' (in Chinese), *J. Softw.*, vol. 22, no. 9, pp. 2059–2074. Sep. 2011.

[32] H. Wang, G. Zhao, D. Qi, and D. Lu, ''Fast incremental learning method for one-class support vector machine,'' (in Chinese), *J. Zhejiang Univ.*, vol. 46, no. 7, pp. 1327–1332, Jul. 2012.

[33] A. Prochazka, O. Vysata, and V. Marik, ''Integrating the role of computational intelligence and digital signal processing in education: Emerging technologies and mathematical tools,'' *IEEE Signal Process. Mag.*, vol. 38, no. 3, pp. 154–162, May 2021.

[34] A. Vaswani, N. Shazeer, N. Parmar, J. Uszkoreit, L. Jones, A. N. Gomez, L. Kaiser, and I. Polosukhin, "Attention is all you need," 2017, *arXiv:1706.03762*.
[35] C. Gou, Y. Zhou, and D. Li, "Driver attention prediction based on convolution and transformers," *J. Supercomput.*, vol. 78, no. 6, pp. 8268–8284, Jan. 2022.
[36] A. Kumar, Z. J. Zhang, and H. Lyu, "Object detection in real time based on improved single shot multi-box detector algorithm," *EURASIP J. Wireless Commun. Netw.*, vol. 2020, pp. 1–18, Dec. 2020.
[37] A. Nazir and M. A. Wani, "You only look once—Object detection models: A review," in *Proc. 10th Int. Conf. Comput. Sustainable Global Develop.*, Cervia, Italy, Sep. 2023, pp. 1088–1095.
[38] P. Wang, A. Zhang, L. Wang, and Y. Dong, "Image automatic annotation based on transfer learning and multi-label smoothing strategy," (in Chinese), *J. Comput. Appl.*, vol. 38, no. 11, pp. 3199–3203&3210, Nov. 2018.

LIAN FEIYU was born in Zhengzhou, China. He received the B.S. degree in information and communication engineering from Zhengzhou University, in 2001, and the Ph.D. degree in computer application technology from Shanghai University, in 2012. Since 2002, he has been a Lecturer with the Henan University of Technology, Zhengzhou. His research interests include the quantitative analysis of terahertz time-domain spectroscopy and the application of THz-TDS to the detection of food quality.

QIN YAO was born in Henan, China, in 1981. She received the Ph.D. degree in engineering from the Graduate School, Chinese Academy of Sciences. She was a Visiting Scholar with the University of Houston. Her research interests include information and signal processing.

FU MAIXIA was born in Henan, China, in 1981. She received the Ph.D. degree with the major of optical engineering. Her research interests include spectral analysis, signal processing, and information theory.